Radiative forcing and temperature response to changes in urban albedos and associated $CO_2$ offsets



2010 Environ. Res. Lett. 5 014005

(http://iopscience.iop.org/1748-9326/5/1/014005)

IOP Publishing Environmental Research Letters
Environ. Res. Lett. **5** (2010) 014005 (11pp) doi:10.1088/1748-9326/5/1/014005

# Radiative forcing and temperature response to changes in urban albedos and associated $CO_2$ offsets

**Surabi Menon[1], Hashem Akbari[1,3], Sarith Mahanama[2], Igor Sednev[1] and Ronnen Levinson[1]**

[1] Lawrence Berkeley National Laboratory, Berkeley, CA, USA
[2] Global Modeling and Assimilation Office, NASA Goddard Space Flight Center, Greenbelt, MD, USA

Received 14 July 2009
Accepted for publication 5 January 2010
Published 21 January 2010
Online at stacks.iop.org/ERL/5/014005

**Abstract**
The two main forcings that can counteract to some extent the positive forcings from greenhouse gases from pre-industrial times to present day are the aerosol and related aerosol-cloud forcings, and the radiative response to changes in surface albedo. Here, we quantify the change in radiative forcing and land surface temperature that may be obtained by increasing the albedos of roofs and pavements in urban areas in temperate and tropical regions of the globe by 0.1. Using the catchment land surface model (the land model coupled to the GEOS-5 Atmospheric General Circulation Model), we quantify the change in the total outgoing (outgoing shortwave + longwave) radiation and land surface temperature to a 0.1 increase in urban albedos for all global land areas. The global average increase in the total outgoing radiation was 0.5 W $m^{-2}$, and temperature decreased by ~0.008 K for an average 0.003 increase in surface albedo. These averages represent all global land areas where data were available from the land surface model used and are for the boreal summer (June–July–August). For the continental US the total outgoing radiation increased by 2.3 W $m^{-2}$, and land surface temperature decreased by ~0.03 K for an average 0.01 increase in surface albedo. Based on these forcings, the expected emitted $CO_2$ offset for a plausible 0.25 and 0.15 increase in albedos of roofs and pavements, respectively, for all global urban areas, was found to be ~57 Gt $CO_2$. A more meaningful evaluation of the impacts of urban albedo increases on global climate and the expected $CO_2$ offsets would require simulations which better characterize urban surfaces and represent the full annual cycle.

**Keywords:** radiative forcing, urban albedo, $CO_2$ offsets

## 1. Introduction

The global radiative forcing associated with land use and land cover change from pre-industrial times to present day due to land albedo modifications is about $-0.2 \pm 0.2$ W $m^{-2}$ (Forster *et al* 2007). This value is small but of opposite sign compared to the 1.6 W $m^{-2}$ forcing from $CO_2$. Regionally, changes to radiative forcing from surface albedo changes can be much larger. For an increase in surface albedo of 0.09, due to an expansion of greenhouse horticulture in southeastern Spain, Campra *et al* (2008) show a strong negative forcing of an average of $-19.8$ W $m^{-2}$. Alpert and Kishcha (2008) suggest that urban areas receive about 8% less annual surface solar irradiance (~12 W $m^{-2}$) than rural areas due to increased aerosol emissions in urban areas. Similar to the urban heat island effect, where urban areas are generally warmer than surrounding rural locations due to urban development (Oke 1982) and indicate a quantifiable increase in surface temperatures (Jones *et al* 1990), radiation budgets

[3] Present address: Department of Building, Civil and Environmental Engineering, Concordia University, Montreal, QC, Canada.

 

in urban areas may be quite different from those in rural locations. These may be due to a variety of factors that include emissions (both GHGs and aerosols), lack of vegetation, urban development and surface albedos.

Here, we examine how surface albedos over urban areas affect radiative forcing. Over 60% of typical US urban surfaces are pavements and roofs (Akbari *et al* 2003) and roofs and paved surfaces constitute about 20–25% to 29–44%, respectively of typical metropolitan US urban surfaces (Rose *et al* 2003). Thus the potential modification to albedos of urban surfaces can have a strong effect on radiative forcing and it becomes useful to quantify this effect since it can to some extent mitigate or delay some of the consequences of warming from $CO_2$ emissions.

Using existing data, Akbari *et al* (2003) suggest that the albedos of roofs and pavements can be increased by at least 0.25 and 0.15, respectively, resulting in an increase of 0.1 in the albedo of urban areas. In order to estimate the benefits that may be obtained from changing urban albedo in terms of $CO_2$ emission offsets, Akbari *et al* (2009; hereafter AK09) derived an equivalency relationship between the radiative forcing of $CO_2$ versus the radiative forcing obtained if the albedos of all urban land areas were increased by 0.1. To obtain the equivalency relationship, the radiative forcing of $CO_2$ was approximated as 0.91 kW $t^{-1}$ of emitted $CO_2$ based on four different modeling studies. For a 0.01 mean increase in global albedo the average global radiative forcing was calculated as $-1.27$ W $m^{-2}$ based on (a) observations, (b) a modeling study and (c) estimated changes in the radiation budget for the Earth–atmosphere system. AK09 found that increasing the reflectance of a roof by 0.25 could offset 64 kg $CO_2$ $m^{-2}$ of roof area (i.e., 16 $m^2$ of cool roof area to offset 1 t of emitted $CO_2$). (Note that for an albedo change of 0.4, a white roof replacing a dark roof, the $CO_2$ offset can be 100 kg $m^{-2}$.) For cool pavements with a proposed albedo increase of 0.15, the emitted $CO_2$ offset was equal to 38 kg $CO_2$ $m^{-2}$ of pavement area (i.e., 26 $m^2$ of cool paved area to offset 1 t of emitted $CO_2$). The estimate of the global emitted $CO_2$ offset potentials for cool roofs and cool pavements is calculated to be about 24 Gt of $CO_2$ and 20 Gt of $CO_2$, respectively, giving a total global emitted $CO_2$ offset potential range of 44 Gt of $CO_2$. Additionally, with a reduction in surface temperature from increased reflectivity, the energy needed for cooling may be reduced, thereby reducing $CO_2$ emissions if the energy supply is from fossil fuels.

The objective of this letter is to quantitatively estimate the effect of urban albedo change on radiative forcing and temperature and then relate the reduction in radiative forcing from enhanced reflectivity to the plausible offsets in $CO_2$ emissions. Here we use a detailed land surface model, the land surface component of the NASA Goddard Earth Observing System Model Version 5 (GEOS-5) global model, to obtain the change in radiative forcing and temperature if the surface albedo of all urban areas were increased by 0.1. We quantify the response of surface variables (surface energy fluxes, radiation and land surface temperature) to a change in surface albedo over global land areas, as well as for a few locations in the US and over the continental US in general.

## 2. Methodology

The land surface model in the NASA GEOS-5 Atmospheric General Circulation Model (AGCM; Rienecker *et al* 2008) is the Catchment Land Surface Model (CLSM; Koster *et al* 2000). We use the CLSM to quantify the effects of an increase in urban albedo on radiative forcing and temperature (the CLSM is run in the offline mode; full coupling between the CLSM and the AGCM was not performed in this study due to the extensive simulation time and computational efforts required). The CLSM computes surface fluxes and surface variables through a comprehensive surface water and energy budget analysis at the land surface. The CLSM uses topographically defined hydrologic catchments as computational elements at the land surface and the model accounts for horizontal heterogeneity of soil moisture within the computational catchment. This approach better characterizes surface properties.

In general, characteristic urban surface albedos are in the range between 0.09 and 0.27 with a mean of ∼0.14 for urban centers (Oke 1988). The 'urban extents mask' of Columbia University's Global Rural–Urban Mapping Project (GRUMP) classifies land as either urban, rural, or neither (e.g., ice-covered) based on the population density and presence of nighttime lights (GRUMPv1 2004). Its 0.5° × 0.5° (0.5° corresponds to ∼50 km in scale) resolution raster was used to identify all urban areas, which comprise about 2.5% of global land area and 0.7% of global surface area.

The CLSM uses a surface albedo parameterization scheme that incorporates climatologies of the visual and near-infrared surface reflectance of the moderate resolution imaging spectroradiometer (MODIS) observations, leaf area index, greenness, sun angle and a snow albedo scheme. To characterize the change in reflectance over urban surface areas, the climatological values of MODIS observations were modified. Monthly climatological values of global snow-free surface reflectance in two broad spectra (UV to visible, 0.3–0.7 $\mu$m; near-infrared, 0.7–5.0 $\mu$m) at a resolution of 2.5′ × 2.5′ used in GEOS-5 was available. A hypothetical surface reflectance data set in which the UV to visible and NIR reflectances of urban areas were each increased by 0.1 to represent the effect of whitening urban surfaces was then created. An example of the original and the modified surface UV to visible reflectance data set is shown in figure 1 for June.

For the simulations used in this work, the CLSM was forced using bias-corrected surface meteorological forcings. The meteorological forcings were obtained from GSWP-2 (second global soil wetness project (Dirmeyer *et al* 2006)). The surface meteorological forcings consist of 3-hourly, 1° × 1° global values for shortwave (downward) (0.15–5 $\mu$m), longwave (downward) (5–120 $\mu$m), 2 m air temperature, 2 m specific humidity, total rainfall, snowfall, convective rainfall, wind, and surface pressure. The CLSM was forced with GSWP-2 forcings and the resulting output is a complete set of surface energy and water balance variables. These include surface hydrological variables, evaporation, surface albedo, land surface temperatures, surface water and energy budgets, amongst other variables. By design, in the offline mode,

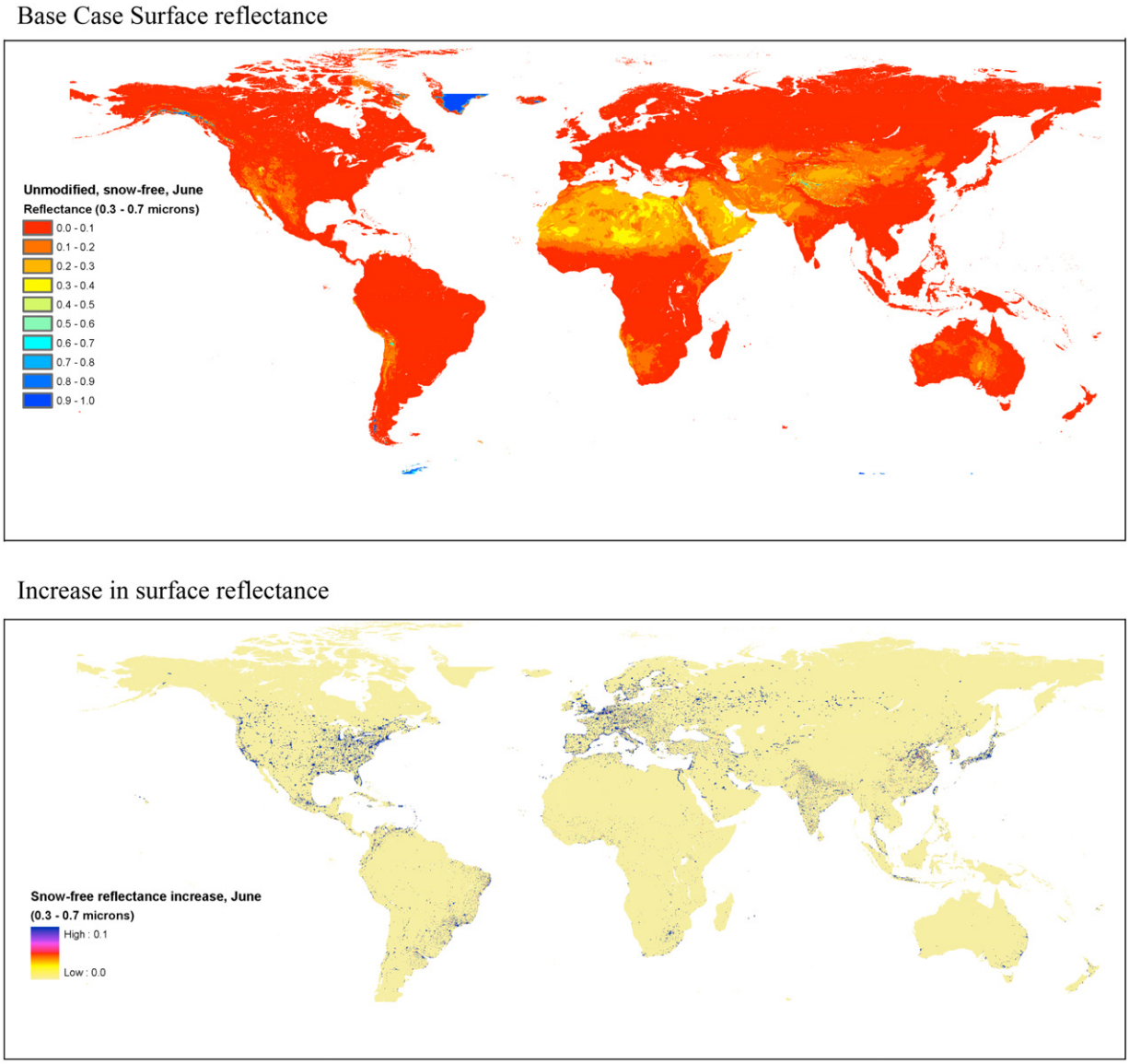


**Figure 1.** Initial values of surface reflectance (UV to visible) and corresponding increase for the selected urban locations for the month of June.

the feedback of the sensitivity of the modifications to the atmosphere is removed. This may allow for the surface terms to be evaluated alone, though any land–atmosphere feedback effects would be missing. Although we use the same 2 m air temperature values for all our simulations, surface variables are allowed to respond to changes in surface albedo, that include evaporative fluxes (latent heat) and land surface temperature (land surface temperature referred to here is the skin or canopy temperature). The offline simulations provide a useful insight on how the changes in surface albedo due to urban build up could affect land surface temperature, and latent and sensible heat fluxes. All values represented are for global land locations, unless indicated otherwise.

## 3. Results

As a first step, the CLSM was forced in the offline mode using bias-corrected GSWP-2 surface meteorological forcings for the period 1984–1995 (i.e. forced with reanalysis data) to evaluate the response of radiative forcing and land surface temperature to the change in imposed surface reflectance. Four sets of simulations were performed and are described in table 1. These include a control simulation labeled as Control (which used the surface reflectances in their original form), and a simulation with the modified surface albedos to mimic urban build up, labeled as Case A. Both Control and Case A simulations were performed on the catchment formulation of the 2° × 2.5°

**Table 1.** Description of the CLSM simulations.

| Simulation | Resolution | Surface albedo | Domain |
|---|---|---|---|
| Control | 2° × 2.5° | Original | Global land locations |
| Case A | 2° × 2.5° | Modified urban areas | Global land locations |
| Control H | 0.5° × 0.5° | Original | Continental US |
| Case AH | 0.5° × 0.5° | Modified urban areas | Continental US |

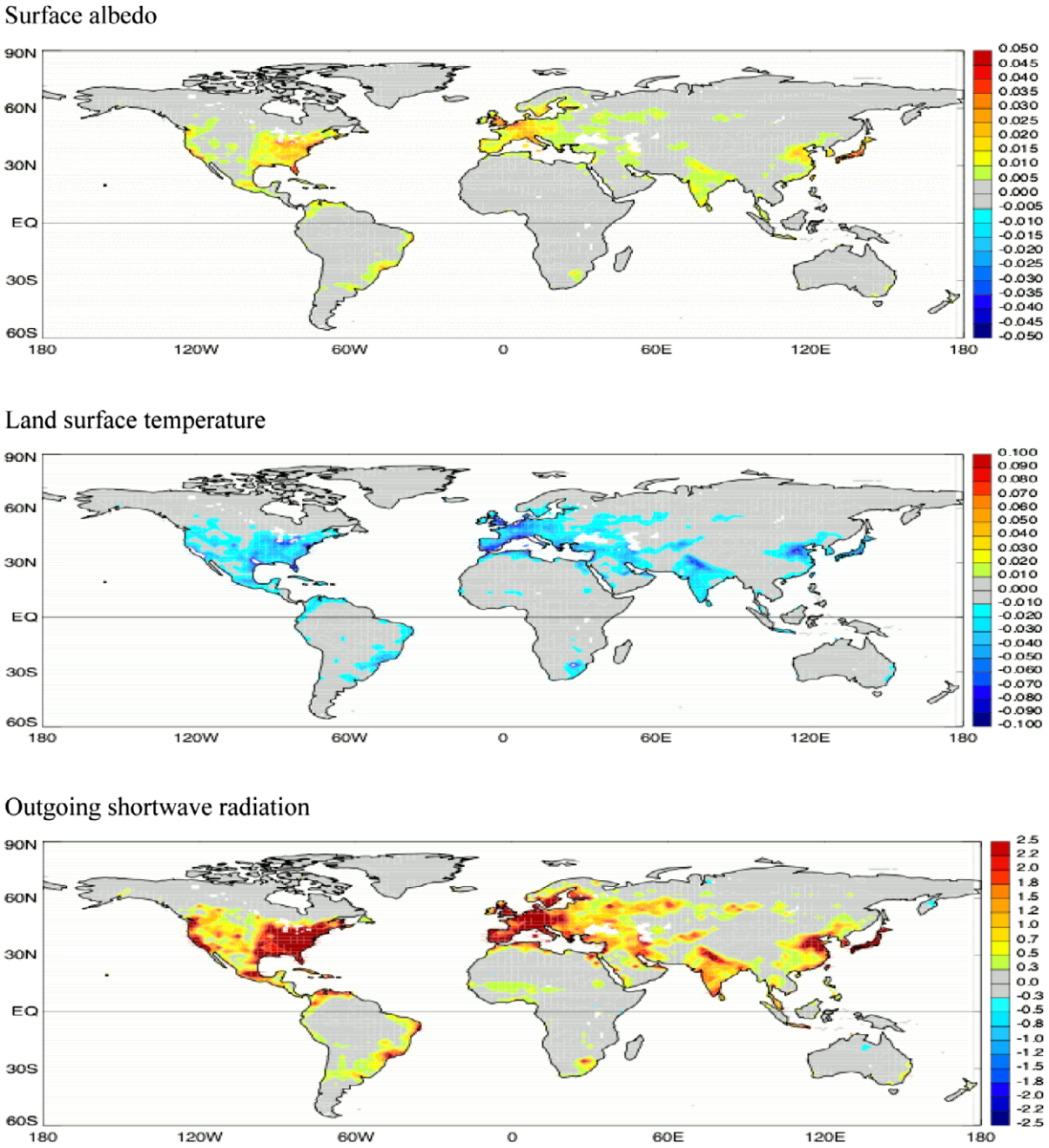


**Figure 2.** Differences between mean values of surface albedo, land surface temperature (in K) and outgoing shortwave radiation (in W $m^{-2}$) for Case A versus Control.

resolution GEOS-5 AGCM. Additionally, two high-resolution (0.5° × 0.5°) simulations similar to Control and Case A were also performed, labeled as Control H and Case AH, respectively. The high-resolution simulations require more intense computing efforts and thus the domain was restricted to the continental US alone. All simulations were performed for three months (June to August) for 12 years. We choose the boreal summer period so that the expected climate response to changes in surface reflectance may be strong due to the larger number of urban areas in the NH and greater probability of occurrence of snow-free conditions.

Figure 2 shows the differences in surface albedo, land surface temperature and outgoing shortwave radiation, between the Case A and Control, obtained from the average values over the simulation period (comprising 36 boreal summer months) for all global land areas. The surface albedo is obtained from the ratio of total outgoing shortwave radiation (computed separately for each spectral band and snow and then aggregated) to incoming shortwave (downward) radiation. As can be seen in figure 2, in general, areas where the surface albedos have increased (top panel) indicate a decrease in land surface temperature (middle panel) and an increase in outgoing shortwave radiation (OSR) (bottom panel) as expected. Changes to the total outgoing (outgoing shortwave + longwave) radiation (shown in figure 3) are dominated by the changes in the OSR field. The maximum

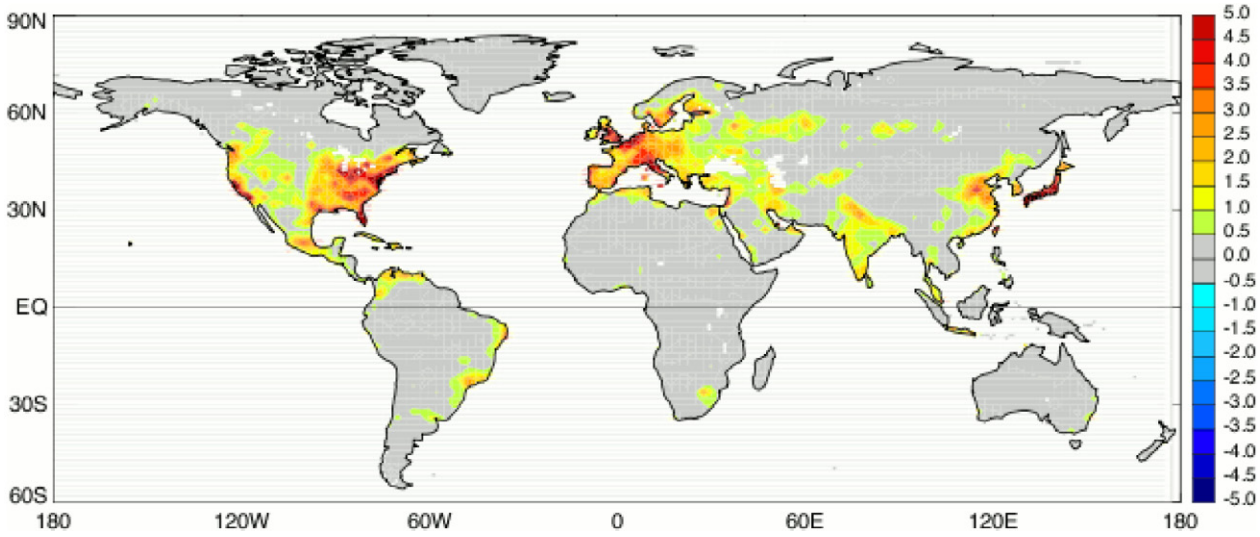


**Figure 3.** Similar to figure 2 but for the total outgoing radiation (in W $m^{-2}$).

increase in OSR was ∼2.5 W $m^{-2}$ and the maximum reduction in land surface temperatures was ∼0.1 K over domains that had an increase in albedo of up to 0.05. The global average reduction in land surface temperature was ∼0.008 K for a global average increase of ∼0.003 in surface albedo. These averages represent all land areas where data were available from the CLSM simulations and not just the selected urban areas where the albedos were increased by 0.1.

Several other fields, including the transpiration rate, surface energy fluxes (sensible heat flux, latent heat flux, ground heat flux), were also examined and the differences were found to be small. The statistical significance of the differences (between Case A and the Control) was calculated for all fields to examine variables that may exhibit a significant difference. The significance, based on a Student's *t*-test, indicates high values (between 0.01 and 0.05) were mainly obtained for the radiation field (OSR) in regions with the surface albedo increases, as expected. Differences for most other variables were not found to be as significant at the 95% confidence interval level.

Most prior studies on changes in surface albedo examine the temperature response to changes in surface albedo. In a recent study, Synnefa *et al* (2008) examined temperature changes from urban albedo changes over Athens, Greece. They found a decrease in the 2 m noon temperature of 0.5–1.5 K, for an albedo change from 0.18 to 0.63, in climate simulations using MM5 (the fifth-Generation NCAR/Penn State mesoscale model). The horizontal resolution for the innermost nested domain resolved the city of Athens at the sub-km scale (0.67 km × 0.67 km). Their ∼1 K change in temperature was for a factor of 3.5 increase in albedo. In a different study, Campra *et al* (2008) examined the temperature response to modified albedos due to greenhouse horticulture in Spain for the 1983–2006 time period. They obtain an annual surface temperature decrease of $-0.029 \pm 0.012$ K for locations with greenhouse horticulture that had surface albedos of $0.28 \pm 0.05$. The pasture surfaces had lower albedos of $0.19 \pm 0.02$ and an annual surface temperature increase of $0.040 \pm 0.013$ K, giving an annual surface temperature decrease of 0.069 K for an albedo increase of 0.09.

For the results shown in figure 2, for a global average surface albedo increase of 0.003, a decrease in land surface temperature of 0.008 K was obtained for the land areas. The land surface temperature response we obtain is higher than that of Campra *et al* (2008). This may be expected since we only consider the boreal summer months. However, the land surface temperature differences from urban albedo changes quantified in this work cannot directly be compared to the results from Synnefa *et al* (2008) due to the domain sizes and time period considered, and since Synnefa *et al* consider the 2 m air temperature response to changes in albedo. In our simulations the 2 m air temperatures were obtained from forcings and were not allowed to respond to changes in surface albedo. Only land surface temperatures, surface energy flux (sensible and latent heat) and radiative flux changes due to the imposed change in surface albedo.

We next examined the variability in the results we obtained. Figure 4 shows the absolute value of the standard deviation based on differences between Case A and Control for the 36 months considered for the variables listed in figure 2. The standard deviation for the change in surface albedo and OSR are smaller than the mean value, but the standard deviation for temperature change is much larger and is close to the mean value. This may be expected since changes to radiative forcing are a direct response to albedo changes, whereas temperature changes may be affected by more than one variable. When the surface albedo increases, net radiation at the surface decreases resulting in a decrease in latent heat fluxes (not shown) and land surface temperatures. However, in the absence of land–atmosphere feedbacks in the offline mode, the resulting effect on land surface temperature is relatively small because the 2 m air temperature from the boundary forcings tends to adjust the effects on land surface temperature changes stemming from modified albedo. As explained in section 2, the 2 m air temperatures are obtained from the GSWP-2 forcings and are not allowed to change

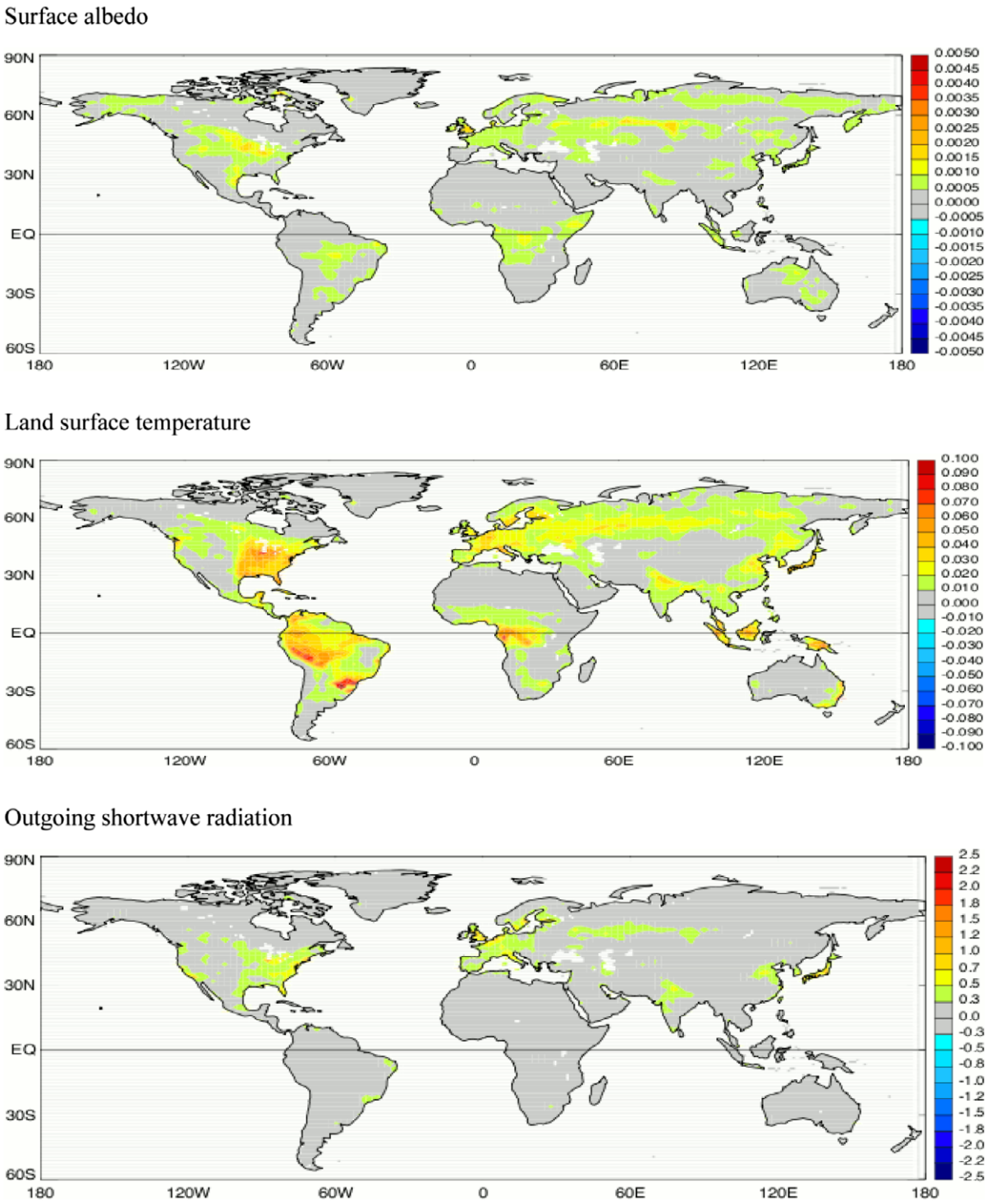


**Figure 4.** Similar to figure 2 but for the standard deviation of the mean differences.

in the simulations; only surface energy fluxes, land surface temperature and radiation can respond to the surface albedo change.

By calculating the ratio of the mean difference between the fields (difference between modified albedo (Case A) and the control run) to the standard deviation of the control run, the signal to noise ratio of the various fields were also examined. This helps determine if the model variability was high and might affect the results obtained. In general, year-to-year variability for the various fields examined appears to be small and thus increasing the sample frequency (runs that are of longer duration) would not modify the results. Most likely the results obtained depend on the strength of the signal and the resolution of the modeling domain that may not represent the true effect of an increase in urban albedo, since urban areas were not explicitly resolved.

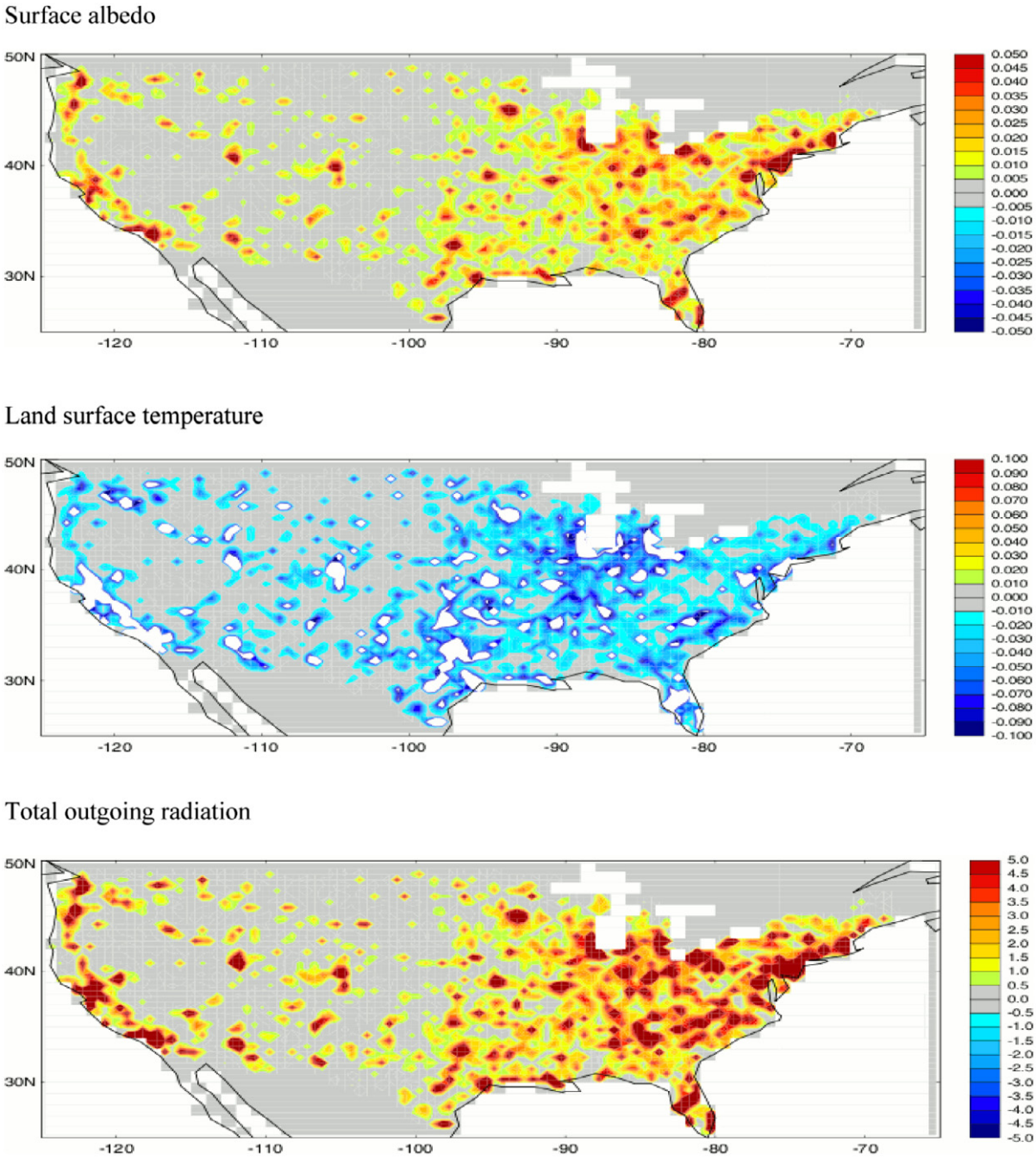


**Figure 5.** Differences between mean values of surface albedo, land surface temperature (in K) and total outgoing radiation (in W $m^{-2}$) for Case AH versus Control H.

Since we wanted to impose realistic changes in urban albedos we did not change the strength of the signal. However, we were able to examine how the results may change depending on the horizontal resolution chosen in the CLSM. These high-resolution (0.5° × 0.5° horizontal resolution) simulations are described in table 1. To adequately resolve urban areas, finer resolutions at the sub-km scale would have been preferable, however resolutions finer than 0.5° × 0.5° horizontal resolution were not feasible in the present study. Mean values of differences between Case AH and Control H for surface albedo, land surface temperature and total outgoing radiation are shown in figure 5 and may be compared to the mean differences shown in figures 2 and 3 for the coarse resolution runs. To quantitatively understand differences in the two sets of simulations based on resolution changes, average values and differences (modified albedo versus control) between simulations for a few variables are listed in tables 2–5 for a few locations (California, Florida, and Texas) and the continental US These allow us to evaluate the local response of the surface variables to the surface albedo change in the urban areas. The choice of locations was based on areas where sufficient data points exist to provide a meaningful sample for the coarse and fine resolutions.

**Table 2.** California results. Mean values and differences between simulations (modified albedo and control) for the coarse (2° × 2.5° horizontal resolution) and fine (0.5° × 0.5° horizontal resolution) model for land surface temperature (K), surface albedo, total outgoing radiation (W $m^{-2}$), outgoing longwave radiation (OLR) (W $m^{-2}$), and outgoing shortwave radiation (OSR) (W $m^{-2}$). Results are based on average values for 12 years of simulations for June to August. The spatial domain chosen was for *California* (36.25°–42.25°N and 115.25°–124.25°W).

| Variables | Control H | Control | Case AH | Case A | Case AH–Control H | Case A–Control |
|---|---|---|---|---|---|---|
| Land surface temperature | 295.08 | 293.64 | 295.02 | 293.59 | −0.06 | −0.05 |
| Surface albedo | 0.195 | 0.179 | 0.205 | 0.194 | 0.01 | 0.015 |
| Total outgoing radiation | 479.3 | 465.1 | 481.3 | 468.2 | 2.0 | 3.1 |
| OLR | 431.9 | 423.2 | 431.6 | 422.9 | −0.3 | −0.3 |
| OSR | 47.4 | 41.9 | 49.7 | 45.3 | 2.3 | 3.4 |

**Table 3.** Florida results. Similar to table 2 but for *Florida* (24.25°–31.25°N and 87.25°–79.25°W).

| Variables | Control H | Control | Case AH | Case A | Case AH–Control H | Case A–Control |
|---|---|---|---|---|---|---|
| Land surface temperature | 300.67 | 300.74 | 300.61 | 300.69 | −0.06 | −0.05 |
| Surface albedo | 0.171 | 0.169 | 0.195 | 0.198 | 0.024 | 0.029 |
| Total outgoing radiation | 495.9 | 495.9 | 500.1 | 501.2 | 4.2 | 5.3 |
| OLR | 463.7 | 464.1 | 463.3 | 463.7 | −0.4 | −0.4 |
| OSR | 32.2 | 31.8 | 36.8 | 37.5 | 4.6 | 5.7 |

**Table 4.** Texas results. Similar to table 2 but for *Texas* (25.25°–36.75°N and 93.25°–106.75°W).

| Variables | Control H | Control | Case AH | Case A | Case AH–Control H | Case A–Control |
|---|---|---|---|---|---|---|
| Land surface temperature | 299.91 | 299.72 | 299.86 | 299.69 | −0.05 | −0.03 |
| Surface albedo | 0.214 | 0.215 | 0.224 | 0.223 | 0.01 | 0.008 |
| Total outgoing radiation | 505.7 | 504.9 | 507.4 | 506.3 | 1.7 | 1.4 |
| OLR | 459.8 | 458.8 | 459.5 | 458.6 | −0.3 | −0.2 |
| OSR | 45.9 | 46.1 | 47.9 | 47.7 | 2.0 | 1.6 |

**Table 5.** US results. Similar to table 2 but for the *US* (25.25°–48.75°N and 67.75°–124.75°W). Also included are the values for the radiative forcing obtained for a 0.01 change in urban albedo (RF01A).

| Variables | Control H | Control | Case AH | Case A | Case AH–Control H | Case A–Control |
|---|---|---|---|---|---|---|
| Land surface temperature | 295.17 | 295.15 | 295.14 | 295.12 | −0.03 | −0.03 |
| Surface albedo | 0.196 | 0.191 | 0.207 | 0.204 | 0.011 | 0.013 |
| Total outgoing radiation | 472.6 | 471.0 | 474.6 | 473.3 | 2.0 | 2.3 |
| RF01A | | | | | 1.8 | 1.8 |
| OLR | 431.8 | 431.7 | 431.6 | 431.5 | −0.2 | −0.2 |
| OSR | 40.8 | 39.3 | 43.0 | 41.8 | 2.2 | 2.5 |

As shown in tables 2–5, with an increase in albedo for all locations an expected decrease in land surface temperature accompanied by an increase in total outgoing radiation is evident. The three locations (California, Florida, and Texas) and the US do indicate higher total outgoing radiation values for a larger increase in urban albedo but the results obtained appear to be resolution independent. A larger decrease in temperature for the higher albedo case was not necessarily evident. In general, it appears that increasing the horizontal resolution from 2° × 2.5° to 0.5° × 0.5° did not significantly affect results in most locations since the fine resolution run was still not explicitly resolving urban surfaces. As illustrated in Synnefa *et al* (2008), resulting climate impacts may need to be examined at the sub-km scale to obtain the full response to the imposed albedo change. Based on the simulations performed at the two resolutions, we suggest that the radiative flux response to urban albedo changes is stronger (compared to the temperature or other fields), as expected, regardless of resolution. However, to obtain a meaningful temperature response, the domain should resolve urban areas and include full feedbacks between the land and atmosphere.

## 4. Discussion

Based on the radiative flux changes we obtained from the CLSM we now examine the $CO_2$ offsets that may be expected. We use RF01A to define the radiative forcing obtained for a 0.01 change in albedo. With the CLSM, as shown in table 5, for an average increase of 0.012 in surface albedo an increase in total outgoing radiation of 2.15 W $m^{-2}$ was obtained for the continental US (for the area between 25.25°–48.75°N and 67.75°–124.75°W). This results in a RF01A value of 1.8 W $m^{-2}$ for the continental US. For all global land areas considered, for an average increase in surface albedo of 0.003, the total outgoing radiation increased by ∼0.5 W $m^{-2}$ (shown in figure 3). The RF01A values based on the changes in radiative forcing to surface albedo for Case A versus Control

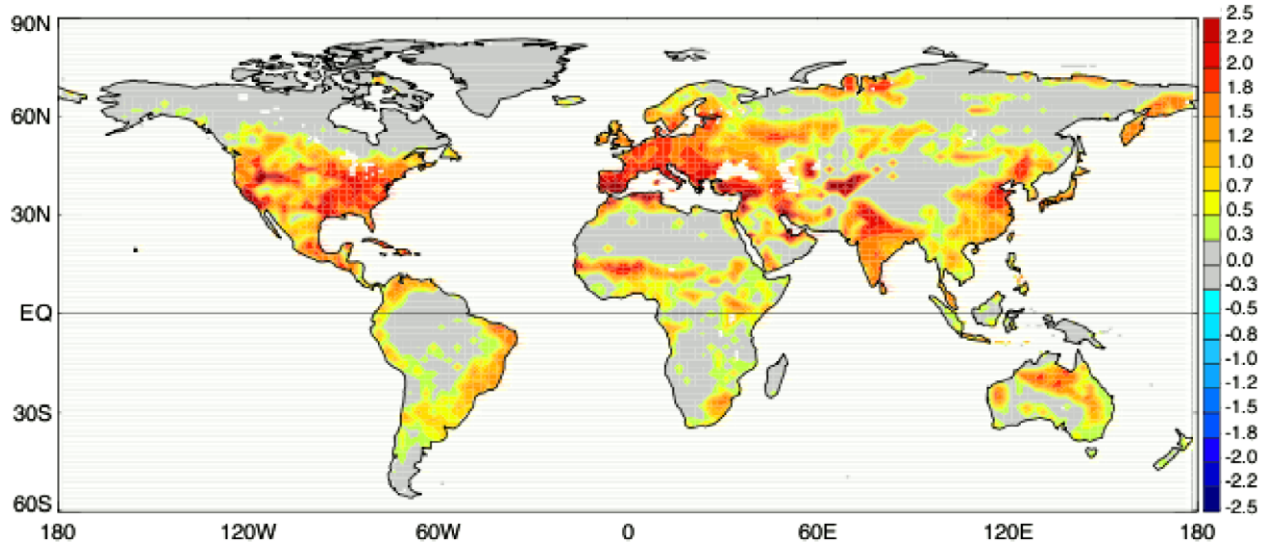


**Figure 6.** Similar to figure 2 but for the radiative forcing per 0.01 increase in albedo. Only values with significant differences in surface albedo were included.

are shown in figure 6. The average RF01A value obtained is 1.63 W $m^{-2}$ (about 10% smaller than the value for the US) for all global land areas.

The simulated response based on the CLSM, in terms of the radiative flux changes to an increase in urban albedo, may be compared to that indicated in AK09. In that study, a global decrease in the top-of-the-atmosphere (TOA) radiative forcing of 1.27 W $m^{-2}$ for a 0.01 increase in solar reflectance of the surface was obtained, based on the annual average global insolation and cloud cover. Some differences between the two RF01A estimates may be expected based on the areas considered (our study was focused on land areas simulated by the CLSM, whereas AK09 considered a global estimate), regional changes in cloud cover and insolation and seasonal changes, since only values for the boreal summer months are included for the simulations with the CLSM which may have a stronger response based on seasonality changes, as also indicated by Campra *et al* (2008). However, both studies indicate a reduction in radiative forcing or an increase in total outgoing radiation for an increase in urban albedo.

For the radiative forcing change of 1.63 W $m^{-2}$ obtained from the CLSM for global land areas, in table 6 we show the equivalent $CO_2$ offsets that may be expected (following the methodology outlined in AK09, see section 5). This comparison may be used to estimate the global land contribution (from surface albedo change in urban areas) to the global equivalent $CO_2$ offsets. For a present-day $CO_2$ concentration of 385 ppm, we estimate the incremental TOA radiative change per tonne of atmospheric $CO_2$ to be 0.91 kW $t^{-1}$ $CO_2$, based on a global average radiative forcing of 3.71 W $m^{-2}$ for the doubling of $CO_2$ (Myhre *et al* 1998). The atmospheric $CO_2$ equivalence for a 0.01 increase in urban albedo is then obtained from the ratio of RF01A (1.63 W $m^{-2}$) to the radiative change per tonne of atmospheric $CO_2$. This value is $-1.79$ kg $CO_2$ $m^{-2}$ urban area. Assuming about 55% of emitted $CO_2$ stays in the atmosphere (Forster *et al* 2007) the emitted $CO_2$ equivalent offset is then $-3.26$ kg $CO_2$ $m^{-2}$ urban area ($-1.79$ kg $CO_2$ $m^{-2}$ urban area/0.55). This value is for a 0.01 change in albedo. To calculate the contribution of urban roofs and pavements to the $CO_2$ offsets, we use the 0.25 increase in roof albedo and 0.15 increase in pavement albedo (from Akbari *et al* 2003) to then estimate the emitted $CO_2$ offsets for roofs and pavements separately. These values are $-82$ kg $CO_2$ $m^{-2}$ roof area and $-49$ kg $CO_2$ $m^{-2}$ pavement area, respectively. If roof areas are 25% of urban areas ($\sim 3.8 \times 10^{11}$ $m^2$) and paved areas are 35% of urban areas ($\sim 5.3 \times 10^{11}$ $m^2$), we then estimate 31 and 26 Gt $CO_2$ offsets for cool roofs and pavements, respectively. As shown in table 6, we obtain a total offset of 57 Gt of emitted $CO_2$ if albedos of urban roofs and pavements were to be increased by 0.25 and 0.15, respectively. For annual changes, we expect a lower number since winter offsets could be lower in some locations.

**Table 6.** Equivalent $CO_2$ offsets based on the radiative forcings obtained for an increase in urban albedos.

| Variable | Values |
|---|---|
| Radiative forcing for a 0.01 albedo increase | 1.63 W $m^{-2}$ |
| *Atmospheric* $CO_2$ equivalent for 0.01 urban albedo increase | $-1.79$ kg $CO_2$ $m^{-2}$ urban area |
| *Emitted* $CO_2$ equivalent offset for 0.01 increase in urban albedo | $-3.26$ kg $CO_2$ $m^{-2}$ urban area |
| *Emitted* $CO_2$ offset for increasing roof albedo by 0.25 | $-82$ kg $CO_2$ $m^{-2}$ roof area |
| *Emitted* $CO_2$ offset for increasing roof albedo by 0.40 (white roof) | $-130$ kg $CO_2$ $m^{-2}$ roof area |
| *Emitted* $CO_2$ offset for increasing pavement albedo by 0.15 | $-49$ kg $CO_2$ $m^{-2}$ paved area |
| Potential emitted $CO_2$ offset for cool roofs | 31 Gt $CO_2$ |
| Potential emitted $CO_2$ offset for cool pavements | 26 Gt $CO_2$ |

The increase in total outgoing radiation and the associated reduction in land surface temperature from an increase in

surface albedo (particularly for the roofs on conditioned spaces) would suggest an indirect benefit of a reduction in demand for energy to cool interior spaces in summer. If this energy supply were from fossil fuels, one might anticipate a reduction in $CO_2$ emissions. Levinson and Akbari (2009) found that retrofitting 80% of the 2.58 billion square meters of commercial building conditioned roof area in the USA (changing the albedos of roofs from 0.20 to 0.55) would result in an annual $CO_2$ net (cooling energy savings minus heating energy penalties) reduction of 6.23 Mt (an average of 2.4 kg $CO_2$ $m^{-2}$ of roof area). The study used building energy simulations, electricity emission factors and building density estimates to calculate energy savings and emission reductions per unit conditioned roof area. Their analysis includes the increase in winter-time heating energy use. A similar analysis is beyond the scope of this letter, but we estimate that in general a cool roof during a typical 20 year life-time will save an additional 50 kg of $CO_2$ $m^{-2}$ of roof area (2.4 kg $CO_2$ $m^{-2}$ of roof area $\times$ 20 years) on an air conditioned building.

## 5. Conclusions

To understand and quantify the effects of changes to radiative forcing and temperature if the albedos of roofs and pavements in urban areas were increased, we performed several sets of simulations with the land component (CLSM) of the NASA GEOS-5 climate model. The simulations were designed to understand the effect of a 0.1 increase in surface albedos over urban areas on radiative forcing and temperature over all global land areas. It was found that the land surface temperature decreased by ~0.008 K for an average increase of 0.003 in surface albedo. These values represent the change estimated from the CLSM for all global land areas (wherever the data were available) for the boreal summer. Other climate variables such as surface energy fluxes (latent and sensible heat), evaporation, etc indicated smaller changes that were not as significant. Only changes to the radiation budget were significant, and an average increase in total outgoing radiation of ~0.5 W $m^{-2}$ was obtained for all global land areas.

The RF01A value obtained (based on the radiative forcing for a 0.01 increase in the surface albedo) is ~1.63 W $m^{-2}$. These values are based on the Northern Hemisphere summer averages for global land locations only. The global average change in radiative forcing for a 0.01 increase in urban albedo derived from theoretical calculations by AK09 was 1.27 W $m^{-2}$ and was based on an annual mean global cloud cover and insolation. AK09 obtained a 44 Gt potential emitted $CO_2$ offset for a 0.25 and 0.15 increase in albedos of roofs and pavements in urban areas. Based on the radiative forcing obtained in this study, the potential emitted $CO_2$ offset for a 0.25 and 0.15 increase in albedos of roofs and pavements in urban areas is about 57 Gt of $CO_2$. If the annual cycle was considered in this work, the offset may be lower. Both studies indicate a qualitatively similar response of a reduction in radiative forcing or an increase in total outgoing radiation for an increase in urban albedo and the values indicate an approximate range in potential emitted $CO_2$ offset that may be expected if urban albedos were increased.

Although it would be ideal to couple the CLSM with GEOS-5 in an interactive manner to understand how land–atmosphere feedbacks may impact the results we obtain, the first task was to understand if the differences obtained between the modified albedo simulation and the control simulation were significant for the variables examined (land surface temperature, evaporation, radiation budgets, etc) and if the model resolution would make a difference. Examining coupled simulations (CLSM coupled to GEOS-5) at a fine resolution requires extensive simulation time and computational efforts that were not feasible for this study, especially since the small perturbations in albedo resulted in small differences that were mainly significant for the radiation fields. Future work will include simulations with a fully coupled global climate model at a high resolution (to explicitly resolve urban surfaces) and will include seasonality so that local climate impacts and expected $CO_2$ offsets may be evaluated more meaningfully. Additionally, we would also estimate the indirect benefits of reduced $CO_2$ emissions due to reduced energy demand (if energy supplied is from fossil fuels) for cooling from reduced surface temperatures, as in Levinson and Akbari (2009).

## Acknowledgments

This work was supported by the California Energy Commission (CEC) through its Public Interest Energy Research Program (PIER), and by the Assistant Secretary for Energy Efficiency and Renewable Energy at Lawrence Berkeley National Laboratory under Contract No DE-AC02-05CH11231. The authors wish to acknowledge the support and guidance from staff of the California Energy Commission Project manager, Guido Franco; and PIER Energy-Related Environmental Research manager, Linda Spiegel. Commissioner Arthur Rosenfeld of the California Energy Commission helped with problem formulation and analysis. We especially acknowledge support from Randy Koster of NASA GSFC, for advice and help with the simulations performed in this work.

## References

Akbari H, Menon S and Rosenfeld A 2009 Global cooling: increasing world-wide urban albedos to offset $CO_2$ *Clim. Change* **94** 275–86

Akbari H, Rose L S and Taha H 2003 Analyzing the land cover of an urban environment using high-resolution orthophotos *Landsc. Urban Planning* **63** 1–14

Alpert P and Kishcha P 2008 Quantification of the effect of urbanization on solar dimming *Geophys. Res. Lett.* **35** L08801

Campra P, Garcia M, Canton Y and Palacios-Orueta A 2008 Surface temperature cooling trends and negative radiative forcing due to land use change toward greenhouse farming in southeastern Spain *J. Geophys. Res.* **113** D18109

Dirmeyer P A, Zhao M, Guo Z, Oki T and Hanasaki N 2006 GSWP-2: multimodel analysis and implications for our perception of the land surface *Bull. Am. Meteor. Soc.* **87** 1381–97

Forster P *et al* 2007 Radiative forcing of climate change *Climate Change 2007: The Physical Science Basis. Contribution of Working Group I to the Fourth Assessment Report of the Intergovernmental Panel on Climate Change* ed S Solomon, D Qin, M Manning, Z Chen, M Marquis, K B Averyt, M Tignor and H L Miller (Cambridge: Cambridge University Press) pp 129–234

GRUMPv1: Center for International Earth Science Information Network (CIESIN), Columbia University; International Food Policy Research Institute (IFPRI), the World Bank; and Centro Internacional de Agricultura Tropical (CIAT) 2004 *Global Rural–Urban Mapping Project (GRUMP)* (Palisades, NY: CIESIN, Columbia University) available at http://sedac.ciesin.columbia.edu/gpw

Jones P D, Groisman P Y, Coughlan M, Plummer N, Wang W-C and Karl T R 1990 Assessment of urbanization effects in time series of surface air temperature over land *Nature* **347** 169–72

Koster R D, Suarez M J, Ducharne A, Stieglitz M and Kumar P 2000 A catchment-based approach to modeling land surface processes in a GCM, part 1, model structure *J. Geophys. Res.* **105** 24809–22

Levinson R and Akbari H 2009 Potential benefits of cool roofs on commercial buildings: conserving energy, saving money, and reducing emission of greenhouse gases and air pollutants *Energy Efficiency* doi:10.1007/s12053-008-9038-2

Myhre G, Highwood E J, Shine K P and Stordal F 1998 New estimates of radiative forcing due to well-mixed greenhouse gases *Geophys. Res. Lett.* **25** 2715–8

Oke T R 1982 The energetic basis of the urban heat island *Q. J. R. Meteor. Soc.* **108** 1–24

Oke T R 1988 The urban energy balance *Prog. Phys. Geogr.* **12** 471–508

Rienecker M M *et al* 2008 *The GEOS-5 Data Assimilation System—Documentation of Versions 5.0.1, 5.1.0, and 5.2.0* vol 27 NASA/TM-2007-104606

Rose L S, Akbari H and Taha H 2003 Characterizing the fabric of the urban environment: a case study of greater Houston, Texas *Lawrence Berkeley National Laboratory Report* LBNL-51448, Berkeley, CA

Synnefa A, Dandou A, Santamouris M and Tombrou M 2008 On the use of cool materials as a heat island mitigation strategy *J. Appl. Meteorol. Clim.* **47** 2846–56